Orissa Journal of Physics
ISSN 0974-8202

Vol. 23, No.1
February 2016
pp. 11-24

Pupil apodization, contrast elevation and spot-size ratio as potential biomarkers

N. K. SHARMA

Department of Physics, Institute of Technical Education & Research, Siksha 'O' Anusandhan University, Khandagiri Square, Bhubaneswar, OR, India
email:nachikk.sharma@gmail.com

Received : 5.*12.2015* ; *Accepted : 13.01.2016*

Abstract: When the entry of a light beam through a pupil is gradually shifted from the centre toward its periphery Stiles Crawford reduction in visibility is observed. In addition to this the retinal visibility can also be governed by generating an interference pattern on the retina. Thus, dependence of visibility on both pupil entry point, and the contrast of the interference pattern can be considered suitable for use as potential biomarkers in early detection of diseases affecting the photoreceptor cones. Likewise, the relation of spot-size of the incident beam to the diameter of the photoreceptor indicating a strong directional coupling of the individual cone photoreceptors to the focused incident beam makes the ratio of the incident spot-size to that of the coupled waveguide mode also a suitable candidate for a biomarker. Finally, modelling Stiles-Crawford effect of the first kind as a pupil apodization, different modulation transfer functions would be obtained for healthy normal eye and an eye with photoreceptor disease. Here in this brief review the theoretical background is illustrated for each case of contrast elevation, spot-size ratio departure and pupil apodization to bring into home the suitability of each of them to be developed into biomarkers for early detection of diseases affecting the photoreceptors.

Keywords: Retinal response, Coherence, Contrast, Stiles Crawford Effect, Waveguiding, Spot-size ratio, Photoreceptor Cone

I. Introduction

In Stiles-Crawford effect of the first kind (SCE I) diminution of visual response of a retina occurs with the change of the entry point of a beam of light from the centre towards the edge of a human pupil [1]. For single pupil entrance point the light, irrespective of its coherence would still show the Stiles-Crawford effect with diminished visibility towards the edge of the pupil [2]. Only when light is incident from opposing points in the pupil can the effect be cancelled as the wavefront slope will be removed with coherent light as shown by recent experiments [3-5]. Here we have theoretically investigated the retinal response to departures from coherence [6], from unit contrast [7], and from perfect spot-size ratio [8].

I.1 Apodization

The change in the effective brightness of a beam is also observed by the pupil apodization [9], so the SCE I diminution of visibility hitherto modelled as pupil apodization [10,11] in spite of the SCE I being retinal in origin [12] is justified [13] as light is assumed to enter into the receptor through a single accepting aperture. Only the amplitude of the incoming wave front at each pupil location is multiplied by the square root of the Stiles-Crawford effect at that pupil location [13] resulting in changes of the modulation transfer function [14] and point-spread function [11]. The coherent response of a grating structure of saw-tooth transmission profile is already studied modelling the SCE I as pupil apodization [6]. Here we take a square wave grating to evaluate the retinal response to departure from coherence.

I.2 Interference Pattern on the Retina

The use of interference fringes for the exploration of the optics of the eye was initiated by Fergus Campbell and Daniel Green [15]. Westheimer also hinted at the phase distribution in Young's interference experiment [16]. Wijngaard worked on mode interference pattern [17]. With the advent of optical coherence tomography [18-20] and adaptive optics [21] retinal image analysis made a tremendous leap. Here, the two-wave interference is adopted to evaluate retinal response in presence of both SCE I and an interference pattern. As the formation of an interference pattern on the retina mimics the SCE I behaviour [4,7], in this study the contrast in the interference pattern is varied to obtain the retinal response.

I.3 Waveguiding of Light

Again as SCE I is expressed mathematically in two different ways: $\eta = 10^{-\rho_{10} r^2}$ and $\eta = e^{-\rho_e r^2}$, where r is the distance in the entrance pupil from the origin of the function and η is the visibility [22], the coefficients (of directionality that measures the width of the pupil apodization) ρ_e and ρ_{10} are related by $\rho_e = \ln 10\, \rho_{10} = 2.3\rho_{10}$. The means and standard deviations [23] for ρ_{10} are: horizontal meridian, $0.048 \pm 0.013 \text{mm}^{-2}$ vertical meridian, $0.053 \pm 0.012 \text{mm}^{-2}$. The directionality involved in the cone-specific [24] nature of this effect led Toraldo di Francia [25] to suggest treating cones as radar waveguides which like cones exhibit directional sensitivity. The evidence of the retina being a microstructure with its cones working as waveguides of light was reported by Enoch [26-28]. Thus SCE I was viewed as being created by a guiding of light into the cone photoreceptors [29]. In this paper, the waveguide coupling and directionality for that waveguide parameter V which supports a fundamental mode is studied. The theoretical values of fraction of normally-incident light power not able to be coupled to a given cone for the fundamental waveguide mode has experimental support from the scanning laser ophthalmoscope measurements [30,31]. As the radius of the cone is restricted [32] between 1-1.5 μm only fundamental mode is taken into coupling consideration. It is shown that the retinal response or the fraction of uncoupled power is governed by the spot-size ratio departure, that is, on the extent by which the incident spot-size and the waveguide mode spot-size differs from each other.

II. Theoretical Modelling

Fourier optics is employed to model the SCE I as a pupil apodization in determining the retinal response in terms of modulation transfer function for spatially incoherent and coherent entering beams. Similarly, the mathematical exploration of the two wave interference pattern on the retina has led to a contrast-controlled retinal response. Finally, the waveguide modelling of a photoreceptor cone supporting a fundamental mode is suggested to evaluate the retinal response to departure from perfect matching of the incident and waveguide mode spot sizes.

II.1 Apodization

A vertical rectangular wave grating with average amplitude a, modulation b, period p and duty cycle α can be expressed as follows [33]:

$$A(x,y) = (a - b + 2\alpha b) + \frac{4b}{\pi}\sum_{n=1}^{\infty}\frac{sin(n\alpha\pi)}{n}cos(n\omega x) \tag{1}$$

where $\omega = \frac{2\pi}{p}$ and x, y are the horizontal and vertical coordinates of space.

Letting $(a - b + 2\alpha b) = C$ and $K_n = \frac{4b\,sin(n\pi\alpha)}{n\pi}$, taking the Fourier transform of Eq. (1) and using two dimensional Dirac delta function $\delta(p,r) = \iint_{-\infty}^{\infty} e^{-i(pq+rs)}dqds$ reduce it to

$$a(u,v) = C\,\delta(u,v) + \frac{1}{2}\sum_{n=1}^{\infty} K_n[\delta(u - n\omega, v) + \delta(u + n\omega, v)] \tag{2}$$

Given that the Fourier transform of the input to the pupil is $a(u,v)$, pupil exit function will be $f(u,v)a(u,v) = a'(u,v)$ for f being the amplitude transfer function which we approximate as follows [14]:

$$f(u,v)=\begin{cases} e^{\frac{-(u^2+v^2)}{\sigma^2}} & \text{if } u^2+v^2<K, \\ 0 & otherwise \end{cases}$$

Where K = 1 for diffraction-limited coherent imaging systems, and K = 2 for diffraction –limited incoherent imaging systems [14] for apodization parameter [23,34] $\sigma = 3.086$.

$$a'(u,v) = e^{\frac{-(u^2+v^2)}{\sigma^2}}\left[C\,\delta(u,v) + \frac{1}{2}\sum_{n=1}^{\infty} K_n[\delta(u-n\omega,v)+\delta(u+n\omega,v)]\right] \quad (3)$$

The image amplitude distribution at the exit pupil is obtained by the inverse Fourier transform of the spectrum $a'(u,v)$ giving rise to $A'(x,y) = C + \sum_{n=1}^{\infty} K_n \int_{-\infty}^{\infty}\int_{-\infty}^{\infty} \frac{[\delta(u-n\omega,v)+\delta(u+n\omega,v)]}{2} f(u,v)\, e^{i(ux+vy)} dudv$

$$= C + \sum_{-\infty}^{\infty} K_n f(n\omega,0)\cos(n\omega x) \quad (4)$$

Substituting back in for C and K_n yields

$$A'(x,y) = a - b + 2\alpha b + \frac{4b}{\pi}\sum_{n=1}^{\infty}\frac{sin(n\alpha\pi)}{n} f(n\omega,0)cos(n\omega x)$$

As $f(n\omega,0) = 0$ for $n\omega \geq 1$ the upper limit n' of n is such that $n\omega < 1$. So, the above equation will be

$$A'(x,y) = a - b + 2\alpha b + \frac{4b}{\pi}\sum_{n=1}^{n'}\frac{sin(n\alpha\pi)}{n}\, f(n\omega,0)cos(n\omega x)$$

Finally, the image energy distribution will be given by the squared modulus of above as

$$\left|A'(x,y)\right|^2 = \left[(a - b + 2\alpha b) + \frac{4b}{\pi}\sum_{n=1}^{n'}\frac{sin(n\alpha\pi)}{n}\, f(n\omega,0)cos(n\omega x)\right]^2$$

For a square wave grating of unit amplitude, as $a = b = \frac{1}{2}, \alpha = \frac{1}{2} \Longrightarrow (a - b + 2\alpha b) = \frac{1}{2}$, the above equation becomes

$$\left[\frac{1}{2} + \frac{2}{\pi}\sum_{n=1}^{n'}\frac{sin(\frac{n\pi}{2})}{n}\, f(n\omega,0)cos(n\omega x)\right]^2$$

where ωx can vary from 0 to π to compute maximum and minimum image energy distribution.

The modulation in the image (for unit contrast in the object) is

$$M = \frac{\left|A'(x,y)\right|^2{}_{max} - \left|A'(x,y)\right|^2{}_{min}}{|A'(x,y)|^2{}_{max} + |A'(x,y)|^2{}_{min}} \tag{5}$$

As the incoherent imaging is linear in image energy distribution, rather than amplitude the image energy distribution and the corresponding modulation equations for incoherent illumination will be given by

$$I(x,y)_{incohernt} = a - b + 2\alpha b + \frac{4b}{\pi}\sum_{n=1}^{n'} \frac{sin(n\alpha\pi)}{n} f(n\omega,0)cos(n\omega x)$$

where a is average intensity and b is modulation.

$As\, f(n\omega,0) = 0$ for $n\omega \geq 2$ the upper limit n' of n is such that $n\omega < 2$ for incoherent illumination [6,35].

$$M_{inc.} = \frac{I_{max} - I_{min}}{I_{max} + I_{min}} \tag{6}$$

II.2 Interference Pattern on the retina

When two plane light waves capable of interference and coming symmetrically from two opposite edges of the pupil meet at a point on the retina, an interference pattern of intensity (I) and phase (φ) is formed with a contrast(m) dependent both on the intensity of the individual light waves $(\mathrm{I}_1, \mathrm{I}_2)$ and the underlying phase difference $[\mathrm{kx} - (-\mathrm{kx}) = 2\mathrm{kx}]$ between them where k denotes the magnitude of the incident wavevector component projected onto the retina.

$$\frac{I}{I_1 + I_2} = 1 + m\cos(2kx)$$

$$\tan\varphi = -\left[\frac{(m-1) - \sqrt{1-m^2}}{(m+1) + \sqrt{1-m^2}}\right](\tan kx)$$

$$m = \frac{2\sqrt{I_1 I_2}}{I_1 + I_2} \tag{7}$$

As seen from Eq. 7, for unit contrast $(m = 1)$ the wavefront slope contained in the phase φ is zero (for $I_1 = I_2$). But, more the intensities of individual beams are unbalanced, more is the departure of contrast from unity leading to a gradual enhancement of wavefront slope at the retina as illustrated in Figure 1.

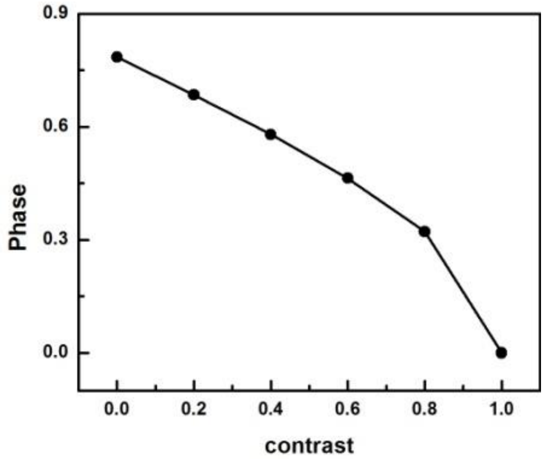

Fig.1. Variation of phase with contrast. More the intensities of individual beams are unbalanced, more is the departure of contrast from unity leading to a gradual enhancement of wavefront slope at the retina.

Hence the enhancement in wavefront slope ($\varphi = 0$, for axial entry and φ is $\frac{\pi}{4}$ for peripheral entry for a fixed retinal location, say, $x = \frac{\lambda}{8}$) with the gradual shifting of the light beam's entry into the eye from the centre to the edge of the pupil modifies the pupil entry point (r) with contrast as follows [4,7]

$$r_{eff} = -\left[\frac{(m-1)-\sqrt{1-m^2}}{(m+1)+\sqrt{1-m^2}}\right] r \tag{8}$$

Where 'r' is the pupil entrance point from the peak of the visibility.

In the absence of the interference pattern the traditional SCE I visibility (η) is given as [23]

$$\eta(r) = e^{-0.115r^2} \tag{9}$$

Where the conventional SCE parameter is 0.115/mm^2.The replacement of r with r_{eff} gives the modified visibility (in presence of interference) as [7]

$$\eta(r,m) = e^{-0.115{r_{eff}}^2} = e^{-0.115\left(\frac{1-m}{1+m}\right)r^2} \tag{10}$$

Eq. 10 shows the dependence of visibility on the contrast in addition to the pupil entry point. This is the required contrast-controlled retinal response function.

II.3 Waveguiding of light

The entire theoretical approach of the model can be outlined as follows: A collimated and spatially filtered He-Ne laser of wavelength 632.8 nm is to be used as a source. This sends out a Gaussian beam whose intensity drops to 14% of its peak value at distance ω_o on either side of the on-axis value. This is then focused on the retina to a spot size of [8]

$$\omega_r = \frac{\lambda f_{eye}}{\pi n_{eye}\omega_o} \tag{11}$$

Where the eye parameters used (in the absence of aberrations) are those of the reduced eye, i.e., a focal length f_{eye}=22.2 mm and a constant index of refraction [36] n_{eye}=1.33. The focused beam couples its power at the retina to the guided modes of a photoreceptor. And a small number of modes share among them the total power carried forward by the photoreceptor. When the entering beam is Gaussian and matches to the location and width of the photoreceptor ($\frac{\omega_r}{\omega_m} = 1$) ($\omega_r$: incident spot size, ω_m: waveguide mode spot size) perfectly, the coupling to the fundamental mode (LP_{01}) becomes the largest. The actual number of possible modes is found from the V number of the waveguide defined by [38]

$$V = \frac{2\pi r_i}{\lambda}\sqrt{n_i^2 - n_s^2} \tag{12}$$

Where n_i and n_r are the indices of refraction of the inner segment (assumed to be uniform) and the surrounding cladding respectively with r_i being the radius of the photoreceptor cone. For fundamental mode, V must be less than V_o = 2.405 which happens if the foveal cones are less than 2.218λ in size [37] and indeed it is so with r_i having values [32] between 1 to 1.4μm.

In this model as the incident beam couples light only to the fundamental mode represented by a Gaussian function of width$2\omega_m$ the fraction of power transmitted to the photoreceptor if incident with its peak value at the photoreceptor axis can be found as [8,38]

$$T(\theta) = \left[\frac{2\omega_r\omega_m}{\omega_r^2+\omega_m^2}\right]^2 \exp\left[\frac{-2\left(\pi n_{eye}\omega_r\omega_m\right)^2\theta^2}{\lambda^2\left(\omega_r^2+\omega_m^2\right)}\right] = \left[\frac{2\omega_r\omega_m}{\omega_r^2+\omega_m^2}\right]^2 \exp\left[\frac{-2\left(\pi n_{eye}\omega_r\omega_m\right)^2 r^2}{\lambda^2\left(\omega_r^2+\omega_m^2\right)f_{eye}^2}\right] \tag{13}$$

.Writing Eq. 13 in terms of the spot size ratio $\left(\frac{\omega_r}{\omega_m}\right)$ (where r is the distance from the on-axis value)

$$T(\omega_r/\omega_m) = \left[\frac{2\frac{\omega_r}{\omega_m}}{1+\left(\frac{\omega_r}{\omega_m}\right)^2}\right]^2 \exp\left[-2\left(\frac{\pi n_{eye}}{\lambda f_{eye}}\right)^2 \left(\frac{\omega_r^2}{1+\left(\frac{\omega_r}{\omega_m}\right)^2}\right) r^2\right] \tag{14}$$

Where $\theta = \frac{r}{f_{eye}}$.

So, $$T(\omega_r/\omega_m) = \left[\frac{2\frac{\omega_r}{\omega_m}}{1+\left(\frac{\omega_r}{\omega_m}\right)^2}\right]^2 \tag{15}$$

Thus the power not able to be coupled can be expressed as

$$1 - T(\omega_r/\omega_m) = 1 - \left[\frac{2\frac{\omega_r}{\omega_m}}{1+\left(\frac{\omega_r}{\omega_m}\right)^2}\right]^2 \tag{16}$$

for the beam passing axially through the pupil (r=0). This is the required retinal response to departure of the spot-size ratio from perfect matching.

III. Results and Discussion

How the retina responds to departure from spatial coherence will be evaluated from the modulation given in Eq. 5 and Eq. 6. Similarly, the response of the retina to departures from unit contrast in an interference pattern formed on the retina will be discussed from the perspective of Eq. 10. Likewise, how the departure from perfect matching of the spot-sizes governs the retinal response will be ascertained from Eq. 16.

III.1 Apodization

The image energy distribution in the images of periodic square wave targets, formed by a human eye apodized with SCE-I under both coherent and incoherent illumination was computed to find out the modulations in the images of periodic square wave targets using Eq. 5 and Eq. 6 respectively. The results are graphically represented in Figure 2. The cut-off frequency determined by the geometry of the cone array is the highest spatial frequency that a normal human eye could resolve if it had perfect optics. So, the fineness of the retinal sampling array imposes a 75 Hz cut-off on square waves that can be delivered to the retina using incoherent light. And for coherent light[6] this will be lower, i.e., 37.5 cycles/deg.

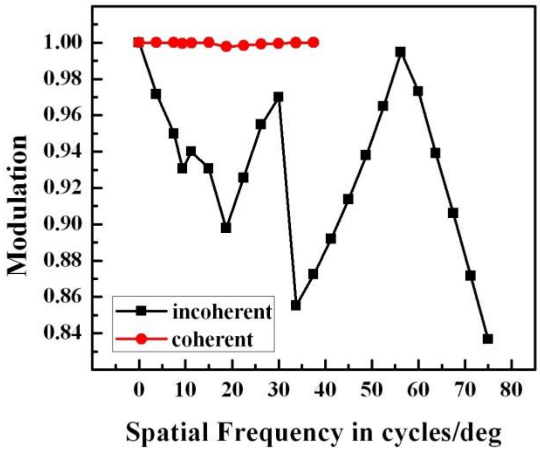

Fig. 2. Variation of modulation with spatial frequency in cycles per degree of visual angle (ω) for both coherent and incoherent illumination for a human eye with SCE I modelled as pupil apodization. With departure from coherence the modulation decreases

From Figure 2, it is evident that the modulation changes only by 0.2 % throughout for coherent entering light. But the modulation registers a variation of as high as 20 % once there is a departure from spatial coherence as is evident from the use of incoherent light. So the retina is quite sensitive to departure from coherence, a whopping 100-fold drop with coherent light changing to incoherent one.

III.2 Interference Pattern on the Retina

The intensity distribution for nil departure from unit contrast (m = 1), maximum departure (m = 0) and for intermediate departures (here, m = 0.5 and m = 0.8 are considered.) is graphically presented in Figure 3 by using Eq. 7.

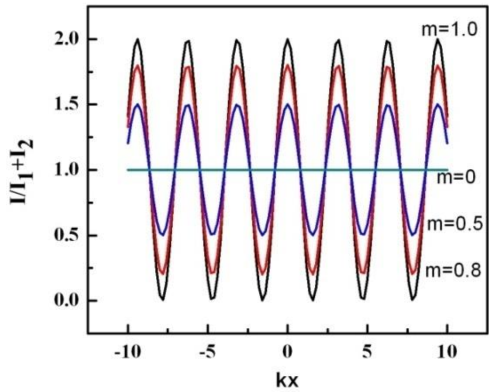

Fig. 3. The intensity distribution for nil departure from unit contrast (m = 1), maximum departure for m = 0, and intermediate departures for m = 0.5 and m = 0.8.

From Eq. 10, $\eta(r,m) = e^{-0.115\left(\frac{1-m}{1+m}\right)r^2}$, it is seen that the visibility depends both on i) to what extent the beams are displaced from the centre of the pupil (r) and ii) the contrast of the interference pattern (m) formed on the retina by the coherent beams. So when visibility, η, is plotted versus the distance of the beam from the centre of the pupil (r) for different values of the contrast (from m = 1 to m = 0 through m = 0.9, 0.8 and 0.5) three interesting observations are noted. First, with no departure from unit contrast the visibility or the retinal response does not depend at all on how the beams are entering through the pupil. Secondly, for maximum departure (m = 0) occurring with the disappearance of the interference pattern from the retina, the retinal response follows in toto the traditional SCE I. And finally, with the gradual enhancement of the departure from zero to maximum the visibility does decrease, but not that quickly with the increase of r compared to the traditional SCE I as illustrated in Figure 4.

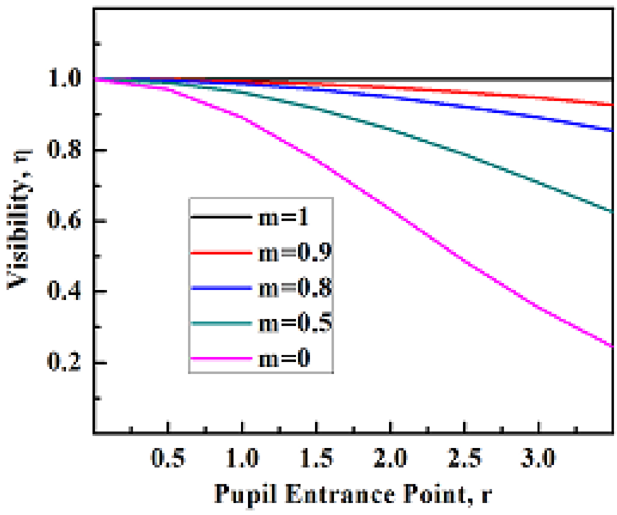

Fig. 4. Variation of visibility with pupil entry point for different departures. Nil departure (m = 1) is independent of pupil entry point, other departures (m ≠ 1) are pupil entry point dependent with maximum departure (m = 0) showing maximum response in the form of more visibility loss.

This we can see more explicitly in Figure 5 by keeping the pupil location fixed at r = 3.5 mm, and gradually increasing the departure from zero to maximum (i.e, m = 1 to m = 0).

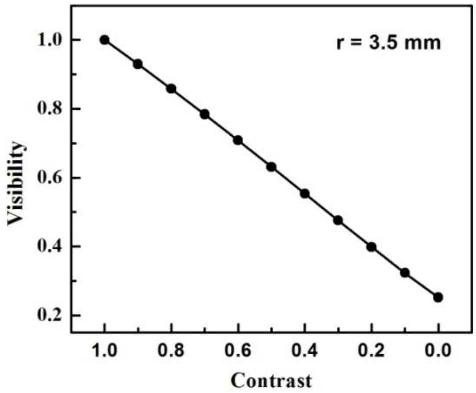

Fig. 5. Variation of visibility with contrast. Gradual enhancement of the departure from zero to maximum (i.e., m = 1 to m = 0) the visibility drops to 24 % of its peak value.

The visibility responds accordingly by decreasing to almost 24 % of its maximum value. With the maximum departure from unit contrast the retinal response takes the traditional SCE route, but with no departure the SCE I becomes totally irrelevant for the retina. For intermediate situations (between $m = 1$ to $m = 0$) the retinal response is controlled by a modified SCE I weakened proportionate to the contrast of the interference pattern on the retina.

III.3 Waveguiding of Light

Using Eq. 16 the fraction of uncoupled power is plotted against spot-size ratio ($\frac{\omega_r}{\omega_m}$) in Figure 6.

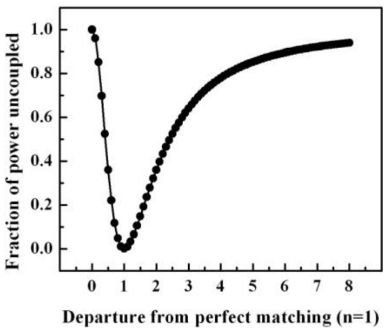

Fig. 6. Response of uncoupled power to departure from perfect matching. At perfect matching condition ($n = \frac{\omega_r}{\omega_m} = 1$), the uncoupled power is zero. The uncoupled power increases with increase of departure in both the direction. With $n = 6$ or $n = \frac{1}{6}$ the uncoupled power drops to 90 % of the peak value.

For perfect matching, $\left(\frac{\omega_r}{\omega_m} = 1\right)$,that is, when the departure is zero, the fraction of uncoupled power attains one hundred percent efficiency. With the increase of the departure the uncoupled power increases and for six-fold departure the uncoupled power becomes 90 % of the peak power achieved for nil departure (or axial entry of the beam).

IV. Conclusion

As retina responds to varying degree to a departure, be it spatial coherence, unit contrast or perfect matching of unit spot-size ratio, the contrast elevation, apodization parameter and spot-size ratio departure can be considered as suitable candidates for biomarkers in detection of diseases specifically affecting the photoreceptor cones.

IV.1 Apodization

We noticed that the modulation in the retinal image did not show any modification in the entire range of the spatial frequency for coherent illumination when the Stiles Crawford effect of the first kind was employed as pupil apodization for a target of square transmission profile. But when the entering light loses its spatial coherence the modulation obtained undergoes modification. This suggests that the retina does respond to departure from coherence that too vigorously with a factor of 100 when coherent illumination is replaced by an incoherent one.

IV.2 Interference Pattern on the Retina

This becomes more evident from the presence of an interference pattern, an attribute of coherence on the retina. With zero departure from unit contrast, the visibility does not diminish. But once the departure starts increasing, the visibility also starts decreasing. Thus the retina responds to departure from unit contrast. And the visibility drops to 24 % of its zero departure value for a fixed pupil entry point of 0.35 cm.

IV.3 Waveguiding of Light

When the incident spot size and the waveguide mode spot size matches, the spot-size ratio is one, departure is zero, coupling of power is 100 % and visibility loss is zero. But with gradual enhancement in the spot-size ratio departure the fraction of power unable to be coupled (or the visibility loss) also increases. Again, a visibility loss of 90 % corresponds to a departure of either 6-fold or 1/6-fold (equivalent to a pupil entry point of 4 mm). This suggests that a pupil entry point of 3.5 mm may point to a loss between 70-80 %, a result reached earlier with departure from contrast. It can be concluded that as departures from perfect spatial coherence, unit contrast, or unit spot-size ratio elicit varying visual response from a human eye, these agencies have the suitability of being used as potential biomarkers for detection of diseases affecting the photoreceptors.

References

[1] WS Stiles and BH Crawford, *Proc. Roy. Soc. B.* **112**, 428 (1933).

[2] LJ Bour and JCM Verhoosel, *Vision Res.* **19**, 717(1979).

[3] B Vohnsen and D Rativa, *J. Vision*. **11**, 1(2011).

[4] S Castillo and B Vohnsen, *Applied Optics*. **52**, A1 (2013).

[5] G Westheimer *J. Opt. Soc. Am. A.* **30**, 1417 (2013).

[6] NK Sharma, *Indian Journal of Science and Technology*. **8**, 906 (2015).

[7] NK Sharma, *Proc. SPIE 9654*, International Conference on Optics and Photonics 2015, 965428-1-7 (June 15, 2015).

[8] NK Sharma and V Lakshminarayanan, *J. Mod. Opt.* **62**, 1278 (2015).

[9] P Jacquinot, P Bougron and B Dossier, *Editions de la Revue d'Optique*. 183 (1949).

[10] H Metcalf, *J. Opt. Soc. Am.* **55**, 72(1965).

[11] JP Carroll, *J. Opt. Soc. Am.* **70**, 1155(1980).

[12] B Vohnsen, *J. Opt. Soc. Am. A*. **24**, 597(2007).

[13] G Westheimer *Prog. Retinal Eye Res.* **25,** 19(2006).

[14] P Artal, *J. Opt. Soc. Am. A.* **6,** 1941(1989).

[15] FW Campbell and DG Green, *J. Physiol.* **181,** 576(1965).

[16] G Westheimer, *J. Opt. Soc. Am..* **50,** 1338 (1958).

[17] W Wijngaard, *Vision Res.* **14,** 889 (1974).

[18] AF Fercher, *J. Biomed. Opt.* **1** 157 (1996).

[19] D Huang et al, *Science*, **254**, 1178(1991).

[20] N Patton et al, *Prog. Retinal Eye Res.* **25,** 99(2006).

[21] A Roorda *J. Vis*. **11** 1(2011)

[22] DA Atchison and A Joblin, *J. Opt. Soc. Am. A* **15**, 2545(1998).

[23] RA Applegate, V Lakshminarayanan, *J. Opt. Soc. Am. A.* **10**, 1611(1993).

[24] F Flamant, WS Stiles, *J. Physiol.* **107,** 187(1948).

[25] G Toraldo di Francia *J. Opt. Soc. Am.* **39**,324(1949).

[26] JM Enoch, GA Fry, *J. Opt. Soc. Am.* **48**, 899(1958).

[27] JM Enoch, *J. Opt. Soc. Am.* **53,** 71(1963)

[28] JM Enoch, *J. Opt. Soc. Am.* **50**, 1025(1960).
[29] AW Snyder and C Pask, *Vis. Res.* **13**, 1115(1973).
[30] D Rativa D and B Vohnsen, *Biomed. Opt. Express*. **2**, 1423(2011).
[31] B Vohnsen and D Rativa, *Biomed. Opt. Express*. **2**,1597(2011).
[32] CA Curcio, KR Sloan, RE Kalina and AE Hendrickson, *Journal of Comparative Neurology*. **292**, 497(1990).
[33] NK Sharma, K Mishra, SK Kamilla, JK Sharma, *IEEE Xplore* In Recent Advances in Photonics (WRAP), 2013 Workshop on , vol., no., pp.1-2, 17-18 Dec. 2013 doi: 10.1109/WRAP.2013.6917630.
[34] NK Sharma, K Mishra, SK Kamilla, JK Sharma, *Adv. Sci. Lett.* **20**, 705(2014).
[35] JW Goodman, *Introduction to Fourier Optics*. Chapter 6, 3rd edition, Viva Books: New Delhi; 2007.
[36] Emsley HH. Visual Optics, 5th ed.; Butterworths: London; 1972; Vol. 1
[37] D Marcuse, *Bell System Technical Journal*. 1997; **56,** 703(1997).
[38] NK Sharma and V Lakshminarayanan, *J. Mod. Opt.* DOI: 10.1080/09500340.2015.1089331. (2015).